AAEC/E383

AAEC/E383

AUSTRALIAN ATOMIC ENERGY COMMISSION

RESEARCH ESTABLISHMENT

LUCAS HEIGHTS

AN ANALYSIS OF POWER TRANSIENTS OBSERVED IN SPERT I REACTORS

PART II: DEPENDENCE OF BURST PARAMETERS ON INITIAL TEMPERATURE AND CORE MODERATION

by

B.E. CLANCY
J.W. CONNOLLY
B.V. HARRINGTON

April 1976
ISBN 0 642 99739 X

AUSTRALIAN ATOMIC ENERGY COMMISSION
RESEARCH ESTABLISHMENT
LUCAS HEIGHTS

AN ANALYSIS OF POWER TRANSIENTS OBSERVED IN SPERT I REACTORS

PART II: DEPENDENCE OF BURST PARAMETERS ON INITIAL TEMPERATURE AND CORE MODERATION

by

B.E. CLANCY
J.W. CONNOLLY
B.V. HARRINGTON

ABSTRACT

The analytical method described in Part I of this series has been applied to the calculation of SPERT I transients performed with higher initial moderator temperatures and also to those performed in a highly undermoderated core. Reasonable agreement has been obtained between calculated and experimental burst data.

National Library of Australia card number and ISBN 0 642 99739 X

The following descriptors have been selected from the INIS Thesaurus to describe the subject content of this report for information retrieval purposes. For further details please refer to IAEA-INIS-12(INIS: Manual for Indexing) and IAEA-INIS-13(INIS: Thesaurus) published in Vienna by the International Atomic Energy Agency.

FEEDBACK; HEAT TRANSFER; REACTIVITY; REACTOR CORES; REACTOR KINETICS; SPERT-1 REACTOR; STEAM; TEMPERATURE DEPENDENCE; TRANSIENTS; VARIATIONS; VOIDS

CONTENTS

(continued)

CONTENTS (Continued)

1. INTRODUCTION

This report extends the analysis of power transients in the light water moderated, plate fuel element SPERT I reactors [Clancy *et al.* 1975] by considering power transients initiated at higher initial moderator temperatures, θ_i, in core B24/32 and from ambient temperatures in the very undermoderated core P18/19. In the latter core, the ratio of the void coefficient of reactivity (expressed in terms of the expansion of water per °C at 20°C) to the neutron spectrum temperature coefficient of reactivity is much larger (0.84) than any other SPERT I core, B24/32 having the next largest ratio (0.32).

The present analysis provides a good test of the validity of two conclusions reached by Clancy *et al.* [1975]. The first conclusion is that a large and positive temperature coefficient of reactivity exists for the light water reflector of the SPERT I reactors. This not only reduces the reactivity effect observed when the whole reactor, rather than the core alone, is heated but also increases the dependence of the overall temperature coefficient of reactivity on temperature. The second conclusion was that steam void formation was not an agent in arresting the power rise in the transient tests performed in the 'B' series of SPERT I cores, but it was of importance for transients in the D12/25 core characterised by values of the initial inverse period α_o greater than 60 s^{-1}. It was expected, therefore, that the large ratio of void to spectrum reactivity effects for core P18/19 would provide a more sensitive test of the validity of neglecting steam void formation in the calculational method.

2. CALCULATIONAL METHODS

The methods for calculating power transients have been described by Clancy *et al.* [1975]. In brief, they involved obtaining core only reactivity coefficients by means of a two-dimensional, four-group diffusion theory representation of the reactor. Both real and adjoint flux solutions were obtained, and perturbation theory was used to obtain reactivity coefficients in representative regions of the core. These coefficients were then weighted by power factors and summed to give a value consistent with the representation of the reactor core by the transient analysis code ZAPP [Clancy, AAEC unpublished report]. ZAPP is a one-dimensional conductive heat transfer code in which a unit cell of fuel alloy, cladding and moderator is explicitly represented. Each such region is

allocated a power density, temperature coefficient of reactivity and thermal properties as part of the ZAPP input.

The boiling heat transfer model of Clancy *et al.* [1975] was again used to describe reactivity feedback when the temperature of the moderator exceeded the saturation temperature at the core centre. In this model, the water channel between fuel plates is divided into fourteen regions; the conductivity of a region is switched to a high value when its temperature exceeds the sum of the initial temperature and the initial sub-cooling divided by the core power factor.

3. TRANSIENTS IN B24/32 INITIATED FROM ABOVE AMBIENT TEMPERATURE

Power burst parameters peak power (P_{max}), energy release at the time of peak power (E_{tm}), and the maximum cladding temperature at the time of peak power (θ_{tm}) were given by Wing [1964] for transients initiated in core B24/32 for moderator temperatures (θ_i) of 20, 40, 60, 80 and 96°C. The calculated reactivity feedback coefficients at these temperatures are, in units of 10^{-5}, 23.3, 27.8, 31.5, 34.6 and 37.3 per degree Centigrade respectively; if this temperature dependence is correct, the product of energy release and reactivity coefficient at all values of θ_i should lie on the same curve when plotted as a function of α_o. Figure 1 shows such a plot and there is quite good correlation of all the energy release data with the exception of that obtained for θ_i = 96°C. From this result, it can be inferred that at temperatures close to saturation, large scale boiling and steam void formation occur before any appreciable feedback from heat conduction processes. This conclusion is supported by the almost exponential rise to peak power shown by these transients, for which values of $\alpha_o E_{tm}/P_{max}$ are close to unity.

Figures 2 to 6 show the comparison between experimental and calculated variations of burst parameters as a function of α_o. Figures 7 and 8 show the ratios of calculated to experimental values of P_{max} and E_{tm}. Although the energy data are mostly contained within the error bounds 0 to -15 per cent, the power data spread is in the range 0 to -40 per cent. One interpretation of this is that the calculated values of energy release are fortuitously in agreement with experiment because of a slower turnaround of the calculated reactor power near P_{max}. Unfortunately, the experimental values of $\alpha_o E_{tm}/P_{max}$, which give an indication of the rapidity with which the power rise is arrested, are anomalously low for values of α_o in the delayed supercritical region [Clancy *et al.*

1975]. Except for those transients with θ_i = 96°C, boiling does not contribute to shutdown according to the experimental temperature data in this range of α_o; either an unknown non-linear (with energy) reactivity feedback mechanism is operating or there is some consistent error between the experimental determination of P_{max} and E_{tm}. The other SPERT I cores analysed by Clancy *et al.* [1975] did not demonstrate these low values of $\alpha_o E_{tm}/P_{max}$ in the delayed supercritical region but, as will be shown later, the same effect occurs in the P18/19 core.

The foregoing discussion does not apply to the transients with θ_i = 96°C, where rather good agreement between calculation and experiment is found for P_{max} and very poor agreement for E_{tm} when $\alpha_o < 10$. However, the calculations are, as might be expected, very sensitive to the temperature at which boiling heat transfer is started, P_{max} changing by 10 per cent for a 1°C change in the boiling temperature.

Experimental values of $\alpha_o E_{tm}/P_{max}$ for these transients approach unity, indicating an almost exponential rise to peak power; the boiling model used in the calculations is unable to reproduce these values for $\alpha_o < 10$, suggesting that in these slower transients the prime shutdown mechanism is the generation of massive steam voids. If this is so, the time delay between the appearance of steam void reactivity feedback and the time at which the coolant attains saturation temperature would appear to be of the order of 100 ms. This is consistent with the delay time of 50-70 ms deduced by Inagaki *et al.* [1972] from pulsed operation of the Hitachi Training Reactor (HTR).

The calculated cladding temperature data appear to be in satisfactory agreement with experimental data, although it is not clear what level of agreement should be looked for in such an intensive parameter. No corrections have been applied to temperature data measured away from the core centre.

4. SPERT I CORE P18/19

This core was basically a mockup of the Army Packaged Power Reactor (APPR). The fuel plates consisted of an alloy of highly enriched UO_2 and stainless steel to which was added 0.12 wt.% B_4C as a burnable poison; this alloy was clad with stainless steel. Eighteen completed fuel plates were then brazed into a fuel box assembly. Table 1 briefly summarises the core component specifications; however, this core has been described more fully by Wing [1964]. The most notable differences

between this and the other SPERT I cores are the high U5 loading/plate and low H/U ratios.

TABLE 1

CORE COMPONENT SPECIFICATIONS

Parameter	P18/19
Water gap (mm)	3.228
Number of fuel elements	19
Fuel plates per element	18
U5 per fuel plate (g)	29
Clad thickness (mm)	0.127
Alloy thickness (mm)	0.508
Metal/water ratio	0.3
H/U ratio	120

4.1 Reactor Physics of the P18/19 Core

The calculational scheme described by Clancy *et al.* [1975] was adopted to obtain a comparison between measured and calculated core physics parameters. The core was not symmetric (see Figure 9) and, to obtain a quarter core representation of the reactor, the outer fuel elements have been indicated by the dotted lines. Table 2 gives the comparison between measured and calculated core parameters. Although there is a large difference between the measured and calculated overall temperature coefficient of reactivity at 20°C, Figure 10 shows that elsewhere, in the temperature range 20 to 90°C, the calculated and measured values of this parameter are in excellent agreement.

TABLE 2

MEASURED AND CALCULATED CORE PARAMETERS

Parameter	P18/19	
	Calc.	Exp.
K_{eff}	1.037	1.034
Max. average power	2.2	not quoted
Void coefficient $1/k.\ dk/dV\ (\%^{-1})$	-3.02×10^{-3}	-3.30×10^{-3}
Overall temperature coefficient $1/k.\ dk/d\theta$ at 20°C	-3.64×10^{-5}	-1.75×10^{-5}
Neutron lifetime ℓ^* (μs)	19.5	14.0

The same data sets and perturbation theory methods were then used to obtain core only reactivity feedback coefficients for use in the reactor kinetics code ZAPP [Clancy, AAEC unpublished report]. The temperature dependence of these data is also shown in Figure 10. Table 3 compares the components of the total reactivity coefficient at 20°C with those calculated by Clancy *et al.* [1975] for other SPERT I cores.

TABLE 3

COMPONENTS OF THE DYNAMIC TEMPERATURE COEFFICIENT AT 20°C

($\times 10^5$)

Component	P18/19	B24/32	D12/25	B16/40	B12/64
	H/U=120	H/U=270	H/U=390	H/U=540	H/U=760
Neutron spectrum ($°C^{-1}$)	-8.3	-17.7	-19.6	-24.5	-29.1
Expansion H_2O ($°C^{-1}$)	-7.0	- 5.6	- 6.6	- 3.6	- 1.3
Total	-15.2	-23.3	-26.2	-28.1	-30.4

4.2 Calculation of Power Transients in Core P18/19

The representation of the reactor by a single cell followed the same procedures described by Clancy *et al.* [1975]. The thermal conductivity and specific heat of the fuel alloy were assumed to be those of stainless steel and were taken from Goldsmith [1961]. Although there appears to be a wide spread in the thermal conductivity data for stainless steels, trial runs of ZAPP showed the power history of even very fast transients to be insensitive to the assumed value of the thermal conductivity; this, no doubt, is a consequence of the thin fuel plate cladding (0.127 mm).

In order to be consistent with the previous calculations of transients in the aluminium fuel plate cores, the experimental value of the prompt neutron lifetime was used, even though a calculated value was available. A limited number of calculations of transients in the super prompt critical region were performed using the calculated lifetime to ascertain the effect of changing this parameter.

4.3 Results of Transient Calculations for Core P18/19

Figure 11 compares calculated and experimental values of the burst parameters P_{max}, E_{tm}, θ_{tm} and θ_{max} (maximum cladding temperature rise).

Figure 12 shows the ratios of calculated and measured peak powers and energy releases; Figure 13 gives calculated and experimental values of the burst shape parameter $\alpha_o E_{tm}/P_{max}$.

From Figure 11, it can be seen that for all $\alpha_o > 25$ the cladding temperature exceeds the saturation temperature of water at the time of the power peak. Figure 12 shows that the ratio of calculated to measured power and energy begins a fairly sharp increase for α_o values greater than thirty. It is inferred from this that steam void formation is becoming an increasingly important shutdown mechanism but is still not the dominant shutdown effect, even for $\alpha_o = 200$.

The variation of the burst shape parameter $\alpha_o E_{tm}/P_{max}$ with α_o, shown in Figure 13, indicates an approximate 25 per cent difference between measured and calculated values. Although the lower experimental values for $\alpha_o > 25$ may be explained by the neglect of steam void formation in the calculation, the discrepancy for α_o values < 25, as in the case of core B24/32, does not offer a ready or plausible explanation.

The calculated temperature data shown in Figure 11 compares quite favourably with the measured data, even to temperature rises as high as 500°C. This indicates that the boiling heat transfer model removes about the right amount of heat from the fuel plates, even if the subsequent conversion of this energy into reactivity feedback is not accurately modelled.

If the calculated neutron lifetime of 19.5 μs instead of the experimental value of 14.0 μs is used in the calculation, the values of P_{max} and E_{tm} increase as indicated by the dotted lines in Figure 11. Below prompt critical, the effect of the neutron lifetime on the power burst will be negligible. It can be seen, therefore, that increasing the value of the neutron lifetime will improve agreement between calculation and experiment in the range of α_o values between prompt critical and the onset of coolant boiling, but beyond that range it will increase the discrepancy between experiment and calculation.

5. DISCUSSION

In this section an attempt will be made to summarise the main conclusions reached from this study of the SPERT I cores. The main topics of interest may be summarised as follows:

- The accuracy and certainty with which reactivity feedback mechanisms have been determined and identified.

- The modelling of heat transfer processes.
- Steam void formation.
- The adequacy of point reactor kinetics in the analysis of SPERT I power transients.

Before discussing these topics, it will be necessary to consider the experimental error associated with the measurement of burst parameters. There is little information in the literature available to the authors on the error assignments for the SPERT I measurements. Obenchain [1969] quotes an uncertainty in the reactor power calibration for the SPERT III oxide core of ± 15 per cent and ± 10 per cent for the SPERT III stainless steel plate core; he implies that these calibrations were obtained from coolant flow rate and temperature measurements. Since SPERT I power calibrations were based on measurements of temperature rise of all the water in the core vessel with the core as the heat source, it is unlikely that the uncertainty in absolute reactor power would be less than for SPERT III; in the following discussion it will be assumed to be ± 15 per cent.

Obenchain also quotes, without elaborating on the source of the scatter, a reproducibility of ± 7 and ± 10 per cent for P_{max} and E_{tm}, respectively, for transients initiated from identical system conditions in the SPERT III oxide core. For lack of any such estimate, the same scatter will be assumed to apply to SPERT I results.

5.1 Reactivity Feedback Mechanisms

The reactivity feedback mechanisms assumed to operate in this analysis are those produced by changes in the neutron energy spectrum caused by an increase in moderator temperature, and changes in moderator density and the metal/water volume ratio of the core caused by changes in moderator and fuel plate temperatures respectively. The reactivity coefficients associated with these effects have been calculated in the simplest possible manner by perturbation theory; the magnitude of the error inherent in this calculation, together with that of the experimental prompt neutron lifetime, will appear as a consistent error in the calculated values of peak power and energy release. The possible magnitude of this error has been assessed by comparison of measured and calculated values of the core void coefficients and overall (core and reflector) temperature coefficients; the conclusion reached is that the error in the reactivity feedback coefficients used in this analysis is

probably in the range ± 10 to 20 per cent. The combination of this consistent error with that of the power calibration will then restrict any conclusions as to the significance of the level of agreement shown between calculation and experimental values of burst parameters in the range ± 30 per cent.

Thus, it is not possible to claim that we have identified all feedback mechanisms; however, the level of agreement obtained with experiment for five cores of widely different neutronic characteristics leads to the belief that the major processes leading to self shutdown have been correctly described. In this connection, it is of interest to note that the power burst properties of core B12/64, which was found experimentally to have a positive void coefficient at the core centre, are reproduced well by the calculational method described.

5.2 Heat Transfer Processes

The principal novelty in the ZAPP method of calculating the transfer of heat from the fuel plate to the water moderator is employed to describe boiling heat transfer after the moderator has reached saturation temperature. Physically, the model describes a situation in which some unspecified process increases the conductivity of the water at any point once the saturation temperature is reached. If this concept is applied to an exponential rise in temperature of the heated surface adjacent to the water, the temperature distribution in the water before the heated surface attains saturation temperature will have a relaxation length of $\sqrt{K/\alpha_o C}$, where K and C are the conductivity and heat capacity of the water respectively. For the range of values of α_o in the SPERT I transients, for which saturation temperatures are attained by the fuel element cladding before peak power, this relaxation length is extremely small; thus it is the temperature gradient established immediately before the water switches to a high conductivity state that determines the heat flux into the 'boiling' region.

Although the mechanism that produces the high conductivity has not been specified, it is tempting to identify it in some way with steam bubble formation; any such void formation, however, will produce a reactivity feedback by means of the void coefficient of reactivity. The best test of the adequacy of the above boiling heat transfer model would come, therefore, from calculating transients in a reactor for which the void volume produced would need to be very large to give a reactivity

feedback equal to that produced by the change in the neutron spectrum with temperature. The core that approaches closest to this condition is B12/64, for which 60 litres of void would be required to produce the same reactivity effect as that produced by raising the moderator temperature from 20 to 100°C.

The calculated burst parameters for this core show good agreement with experiment over the range of α_o (10-100), for which the cladding temperature at the core centre reaches saturation at or before peak power. It is concluded that the increase in the rate of reactivity feedback, once core boiling occurs, is caused by a change in heat conduction processes rather than by void formation. The validity of this conclusion for cores with much larger void coefficients of reactivity will be examined in the next section.

5.3 Steam Void Formation

Of the five SPERT I cores analysed in this series, only D12/25 showed a gross departure from agreement between calculation and experimental values of burst parameters (Figure 14). In an attempt to obtain a semi-quantitative understanding of why this core alone exhibits this behaviour, it was assumed that, for transients characterised by α_o values greater than 40 s^{-1}, steam void formation contributed to reactor shutdown. At the time of peak power for a transient, characterised by α_o = 40 s^{-1}, the calculated cladding temperature at the core centre was 150°C. A trial series of negative ramp reactivity additions was started at this temperature in the ZAPP calculations in an attempt to match the experimental data. (A linear ramp is the only one possible in ZAPP, so this choice does not reflect on any physical reasoning.) A ramp of -2.0 $\delta k/k\ s^{-1}$ was found to reproduce the experimental data to the time of peak power quite well (dashed lines in Figure 14). The burst asymmetry, characterised by the ratio of the total energy release to the energy release at peak power, is also reasonably reproduced, at least for values of α_o less than 200 s^{-1} (Figure 15).

The average void coefficient of reactivity for D12/25 was approximately -0.6 $\delta k/k\ cm^{-3}$ and the maximum was -0.9 $\delta k/k\ cm^{-3}$. A value of -0.8 $\delta k/k\ cm^{-3}$ was assumed for the core volume over which steam was formed; from this value and from the ramp of -2.0 $\delta k/k\ s^{-1}$, a steam void growth rate of 2.5 x 10^5 $cm^3\ s^{-1}$ was deduced. This simple picture of steam void formation, that is of steam voids growing at a rate of 2.5 x 10^5 $cm^3\ s^{-1}$ once the central cladding temperature exceeded 150°C, was

then applied to the remaining four cores.

For core B12/64, it was found that although the temperature of 150°C is reached before peak power for all α_o greater than 40 s^{-1}, the small value of the void coefficient (-0.03 $\delta k/k\ cm^{-3}$), in conjunction with the assumed void growth rate, produced a much smaller reactivity feedback rate than the ZAPP boiling heat transfer model. (For a transient of α_o = 100, close to the time of peak power the latter is producing negative reactivity feedback at a rate of -0.7 $\delta k/k\ s^{-1}$, compared with -0.08 $\delta k/k\ s^{-1}$ from the assumed steam void growth rate.)

For both B24/32 and P18/19, the temperature of 150°C is not attained before peak power for transients characterised by α_o values less than 100, so that steam void formation would mostly influence the shape of the post peak power history, for which experimental information is not available. The rate of insertion of negative reactivity from steam void growth would be comparable to D12/25 for both these cores.

Core B16/40, although reaching 150°C at the time of the power peak for a transient having an α_o of about 30 s^{-1}, will produce only one quarter of the steam void reactivity feedback rate of D12/25 (it is assumed that rate of void growth is the same for each core) because of its smaller void coefficient. This rate is still large enough to influence the course of transients for which α_o exceeds about 50 s^{-1}, but there is insufficient experimental data in this region to conclude that the assumed steam void growth rate is correct.

It is suggested that the above discussion offers a plausible if oversimplified explanation of the importance of differences in steam void formation in SPERT I cores. The validity of the model could be more fully explored by a detailed comparison of calculated and measured power burst shapes, but sufficient data is not available in reports relating to SPERT experiments.

5.4 Point Reactor Kinetics

The SPERT I cores discussed in this report were all small and the transients were initiated by rapid ejection of a central control rod; it may be reasonable to suppose that during the transient measurements space dependent effects may arise, and these will not be included in the point kinetic model of the reactor used in ZAPP. One way of looking at this question is to compare the ratios of centre cladding temperature rise and core energy release as a function of α_o for experiment and

calculation. If both have the same general form, the spatial flux effects during the transients will be small. Such a comparison made for the present work does not give rise to doubts about the adequacy of the point reactor model.

6. CONCLUSIONS

A method has been presented for analysing power transients following step and ramp rate reactivity additions in light water moderated, plate fuel element reactors under conditions of zero coolant flow. The results of this method, when applied to SPERT I reactors, give sufficient agreement with experimental burst parameters to give confidence in the application of the method to similar reactor cores.

A better physical insight into the processes occurring during such transients would require that the experimental data, particularly reactor power calibration data, be obtained with better accuracy.

7. REFERENCES

Clancy, B.E., Connolly, J.W. & Harrington, B.V. [1975] - An analysis of power transients observed in SPERT I reactors. Part 1: Transients in aluminium plate type reactors initiated at ambient temperatures. AAEC/E345.

Goldsmith, A. [1961] - Handbook of thermophysical properties of solid materials, vol.II. MacMillan, New York.

Inagaki, K., Doi, A., Yamamoto, H. & Kitaguchi, H. [1972] - Boiling of water during HTR pulse operation. *J. Nucl. Sci. Technol.*, 9 (1) 64-66.

Obenchain, C.F. [1969] - PARET - A program for the analysis of reactor transients. IDO 17282.

Wing, A.P. [1964] - Transient tests of the fully enriched, stainless steel plate type P core in the SPERT I reactor. IDO 17011.

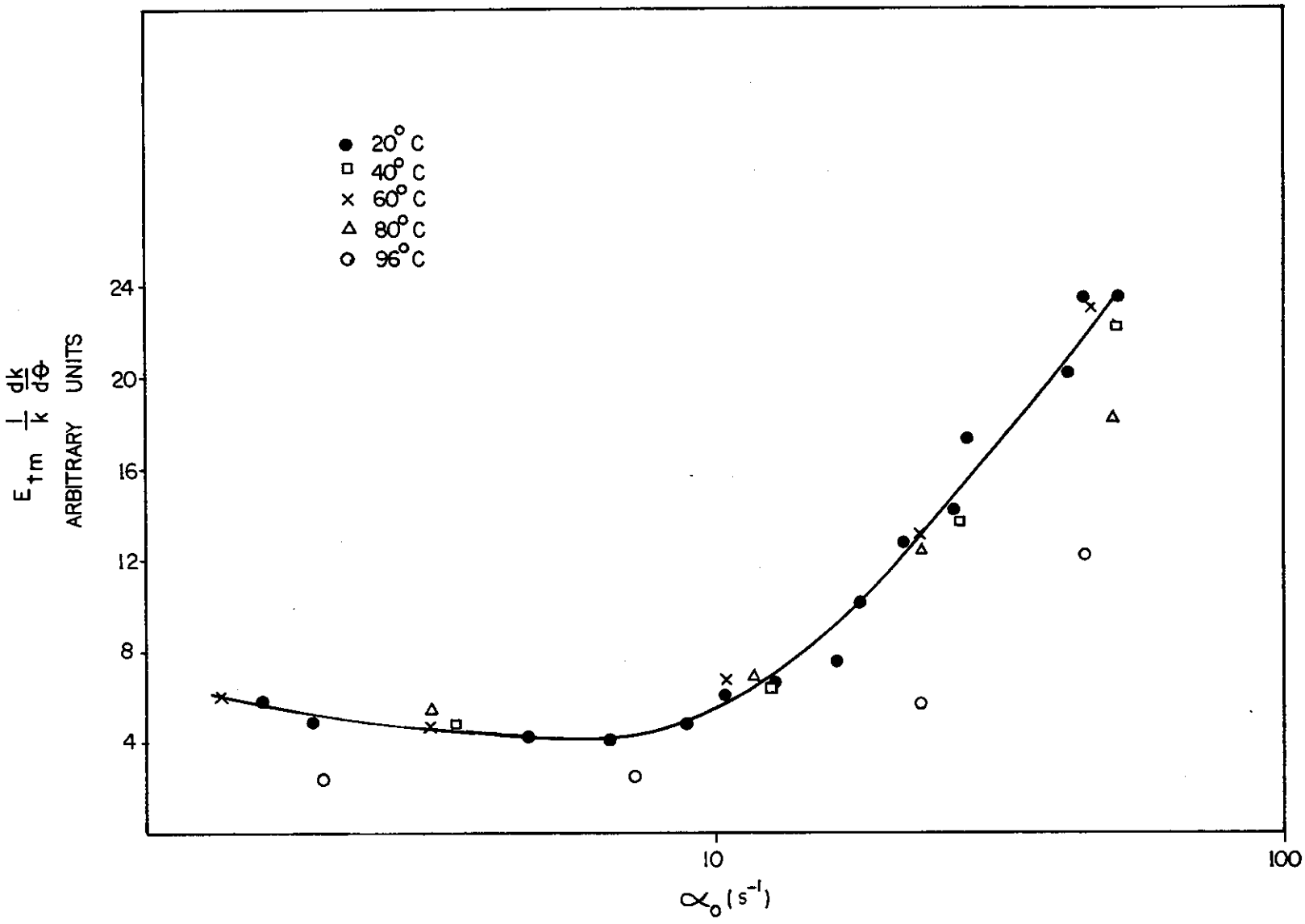

FIGURE 1. CORRELATION OF B24/32 ENERGY RELEASES BY TEMPERATURE DEPENDENT REACTIVITY FEEDBACK COEFFICIENTS

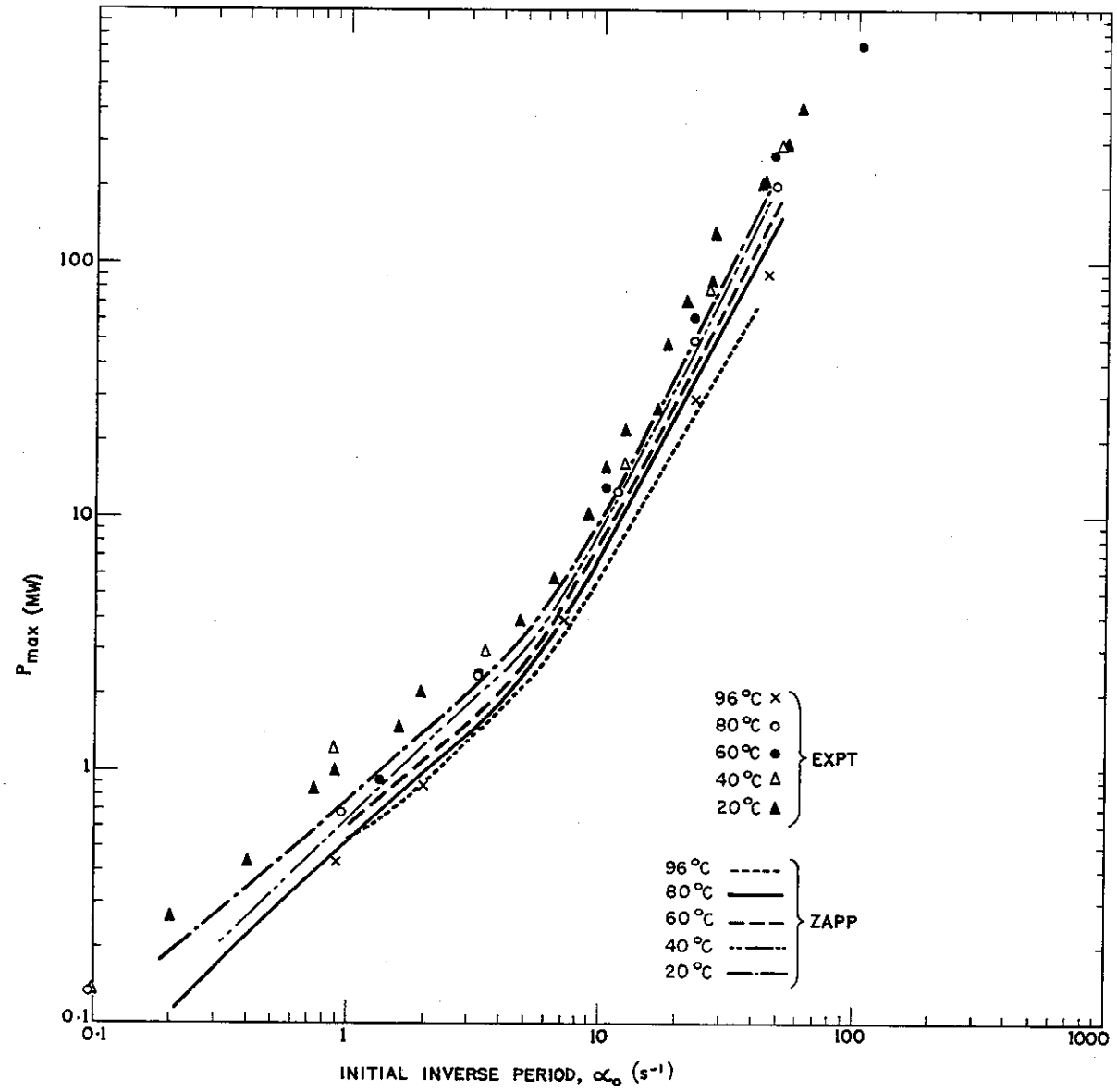

FIGURE 2. CALCULATED AND MEASURED PEAK POWER, CORE B24/32

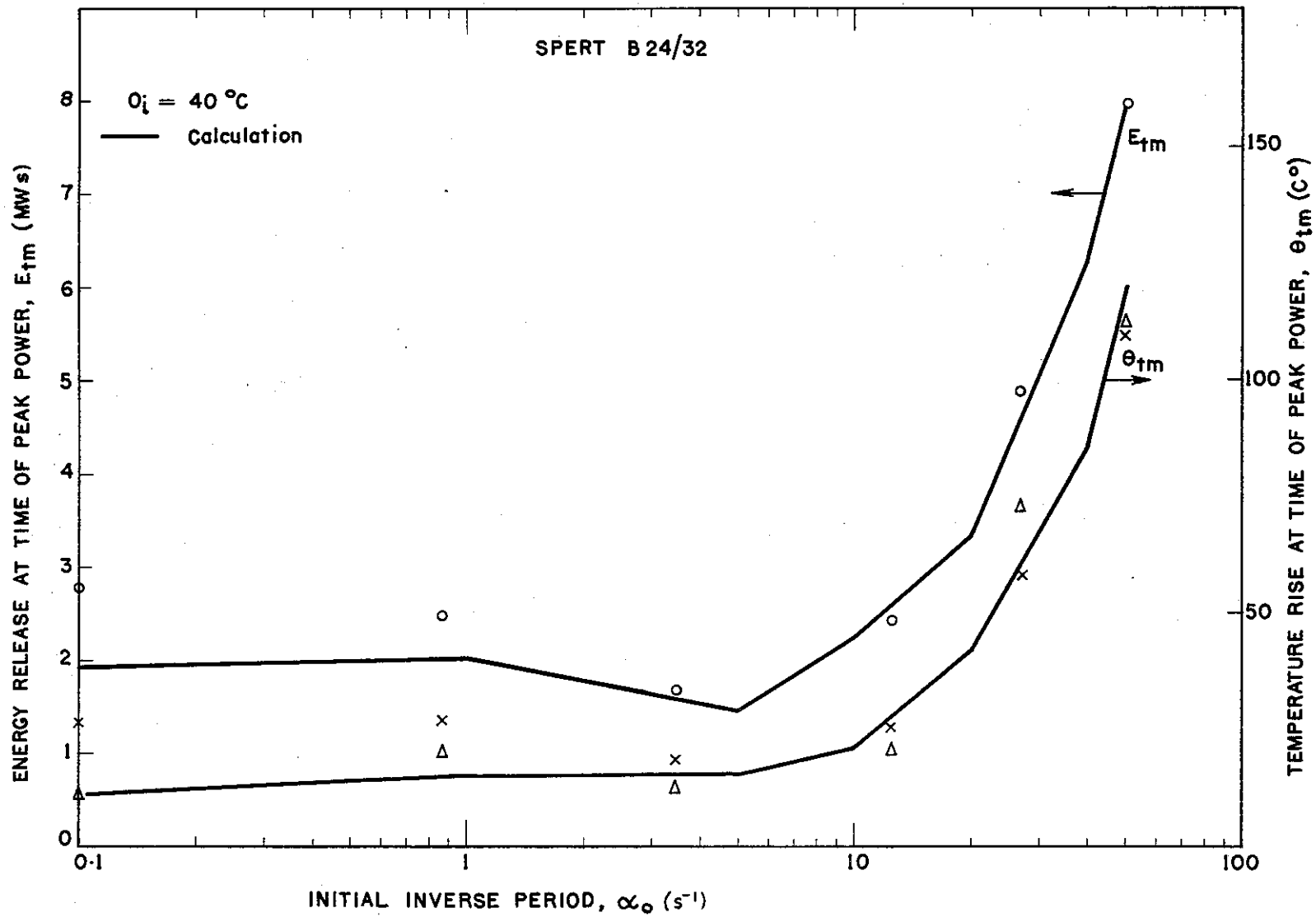

FIGURE 3. CALCULATED AND MEASURED ENERGY RELEASES AND FUEL PLATE TEMPERATURES, CORE B24/32, FOR AN INITIAL TEMPERATURE OF 40°C

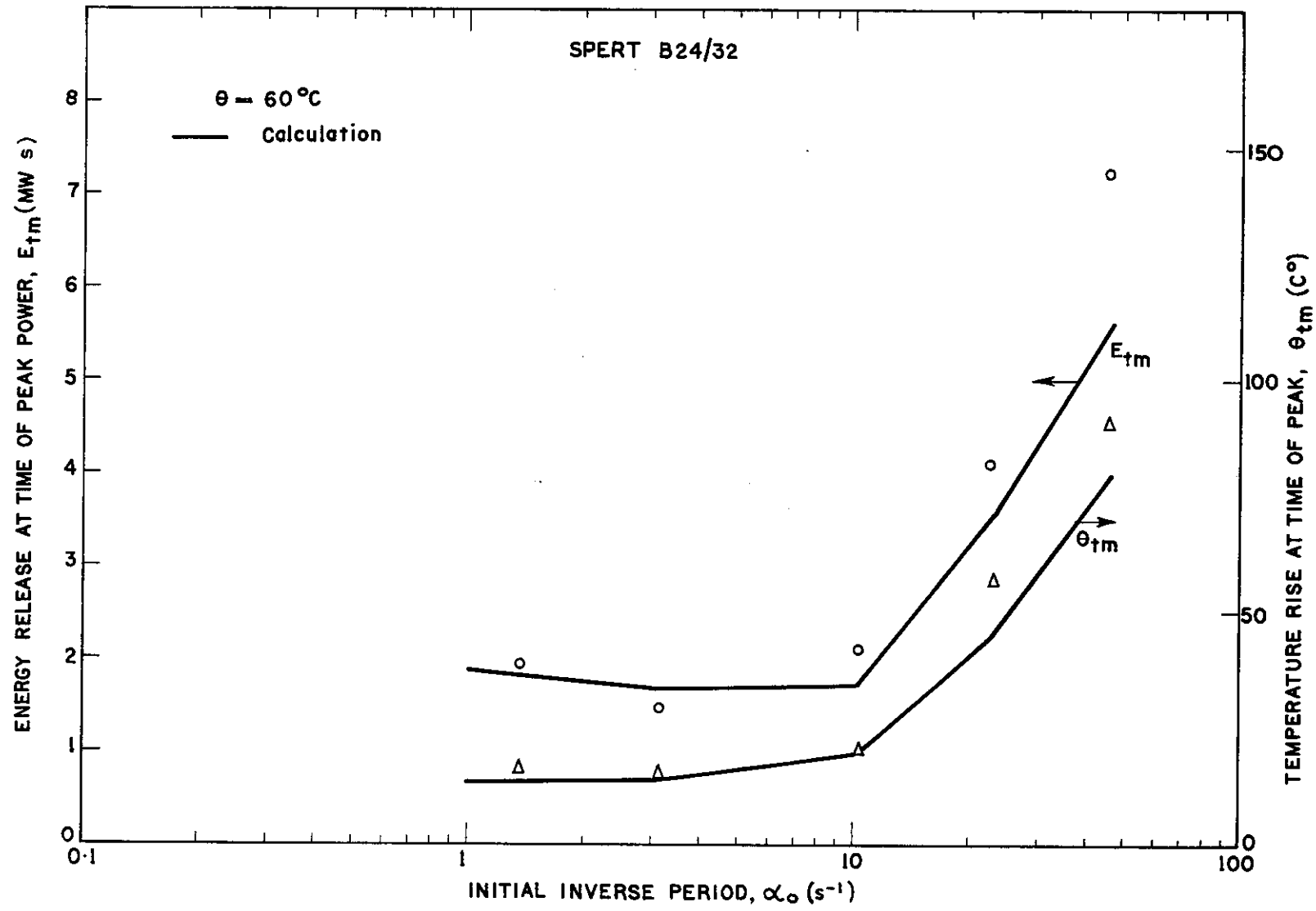

FIGURE 4. CALCULATED AND MEASURED ENERGY RELEASES AND FUEL PLATE TEMPERATURES, CORE B24/32, FOR AN INITIAL TEMPERATURE OF 60°C

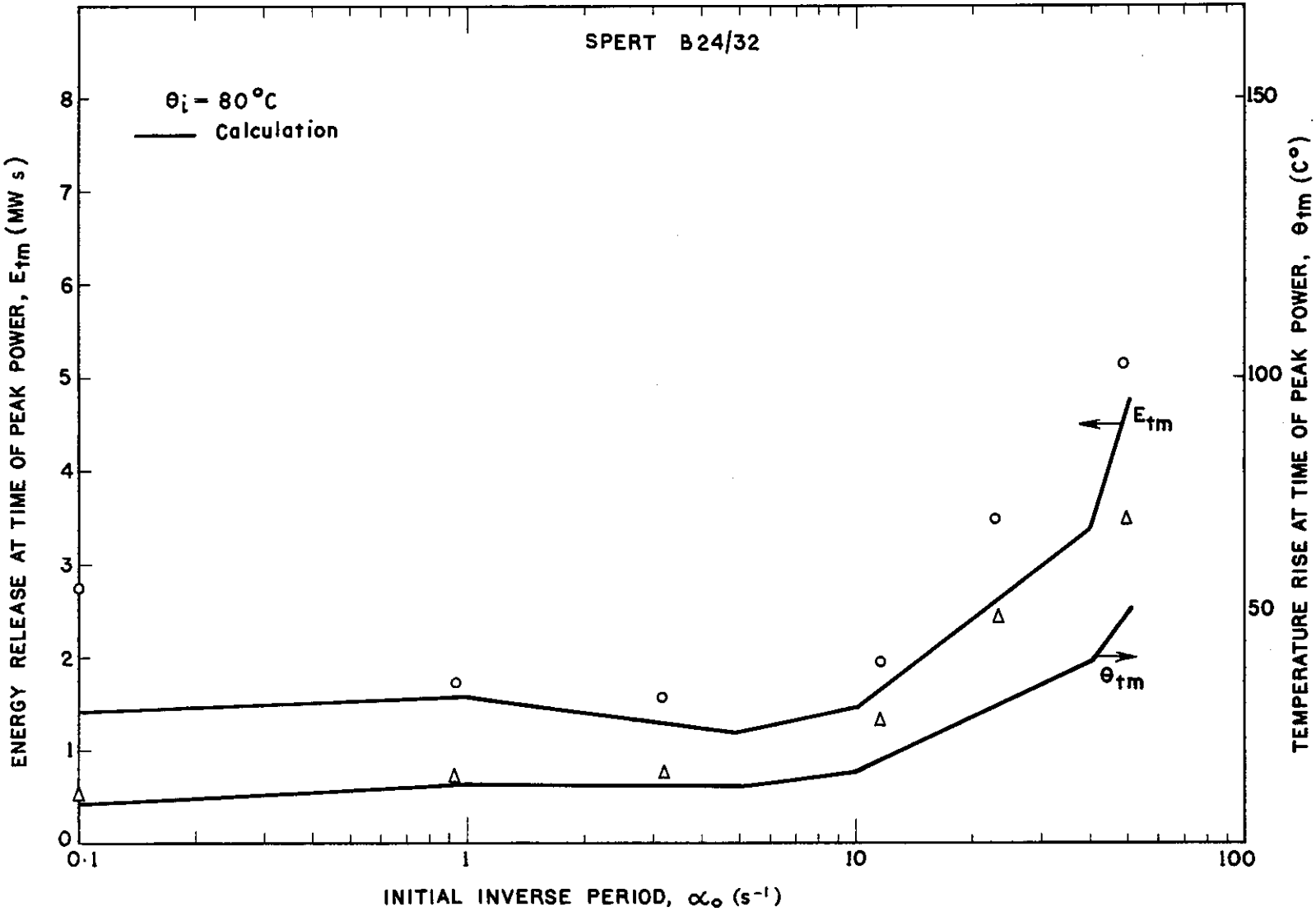

FIGURE 5. CALCULATED AND MEASURED ENERGY RELEASES AND FUEL PLATE TEMPERATURES, CORE B24/32, FOR AN INITIAL TEMPERATURE OF 80°C

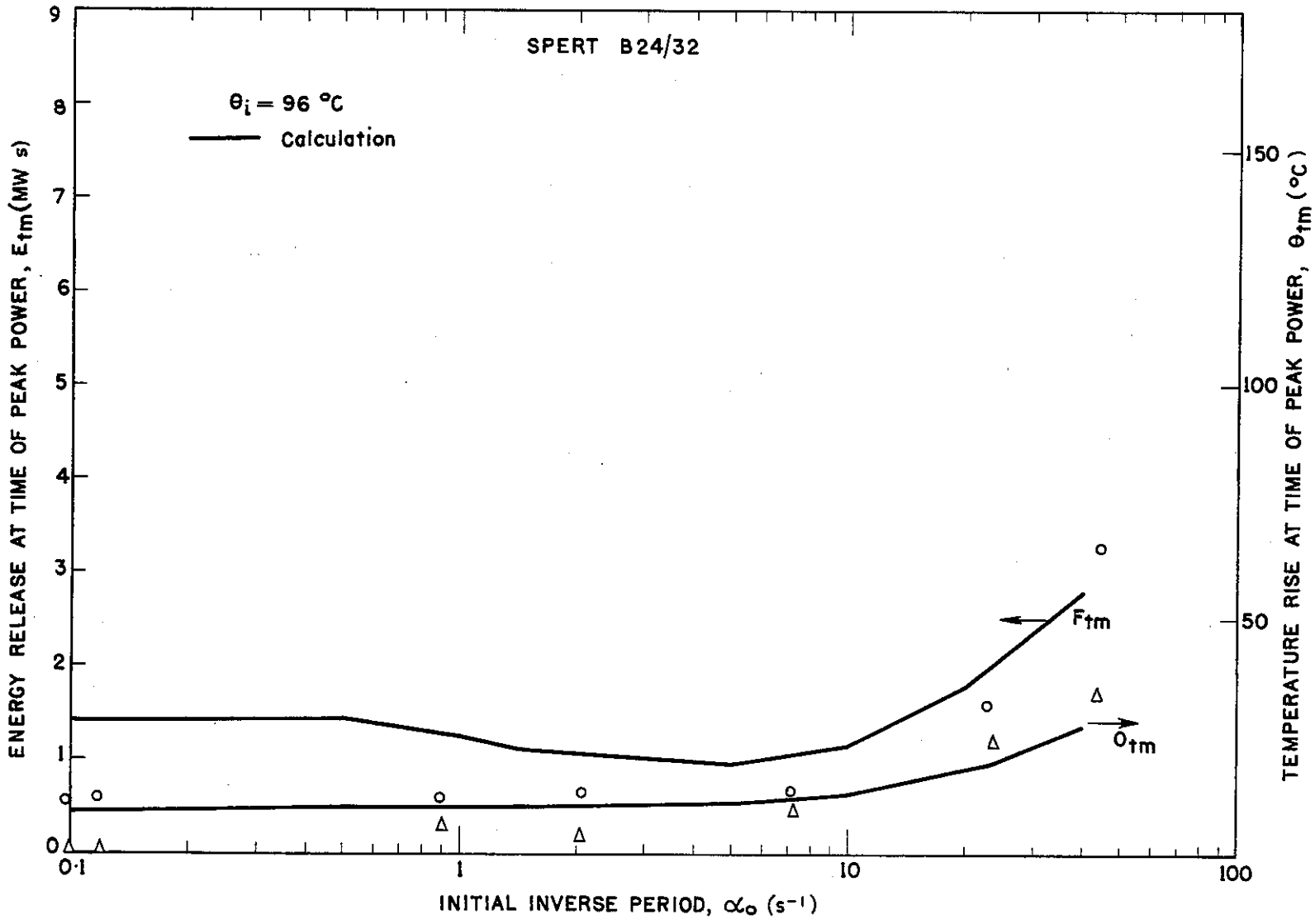

FIGURE 6. CALCULATED AND MEASURED ENERGY RELEASES AND FUEL PLATE TEMPERATURES, CORE B24/32, FOR AN INITIAL TEMPERATURE OF 96°C

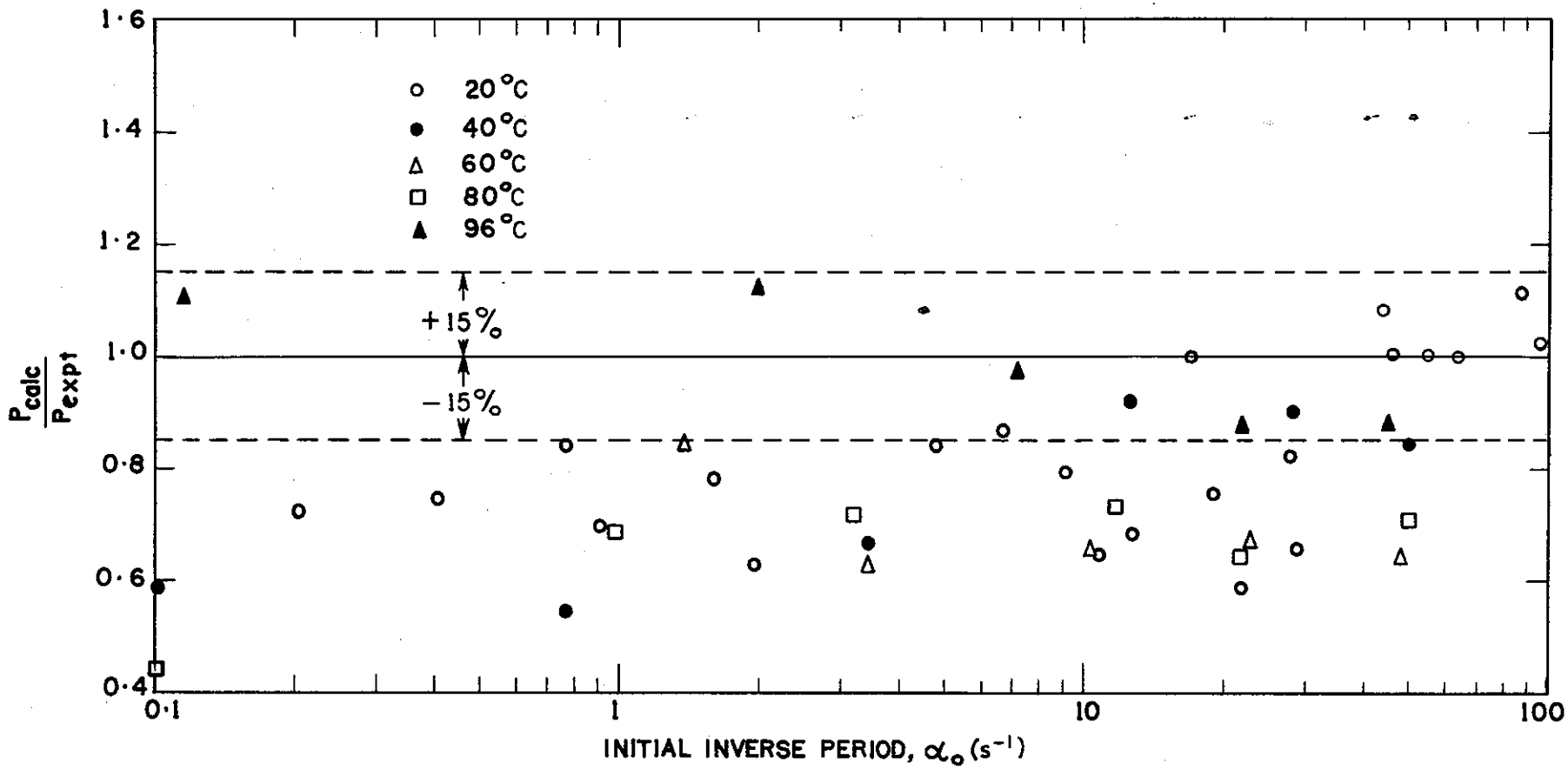

FIGURE 7. RATIOS OF CALCULATED AND MEASURED PEAK POWERS, CORE B24/32

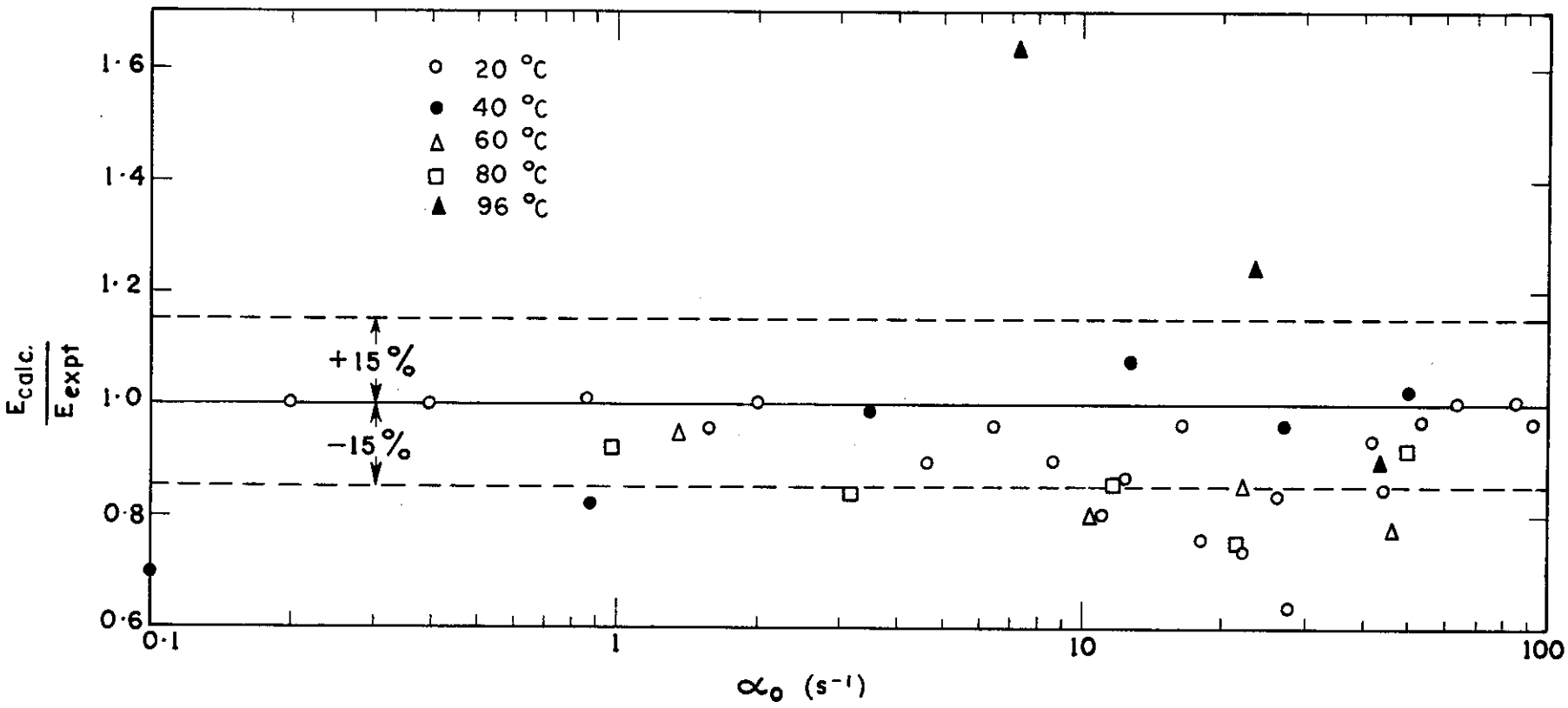

FIGURE 8. RATIOS OF CALCULATED AND MEASURED ENERGY RELEASES, CORE B24/32

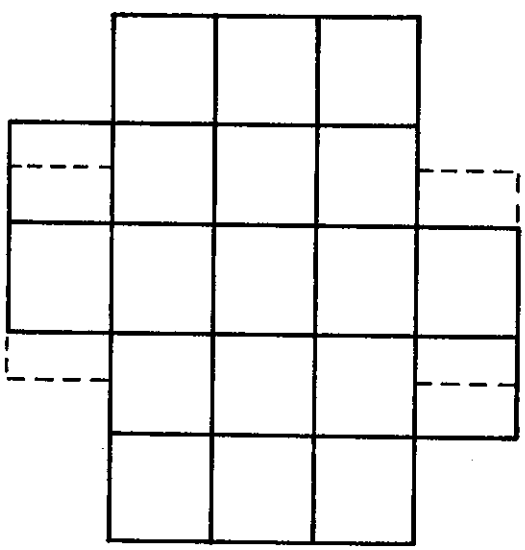

FIGURE 9. P18/19 CORE GEOMETRY

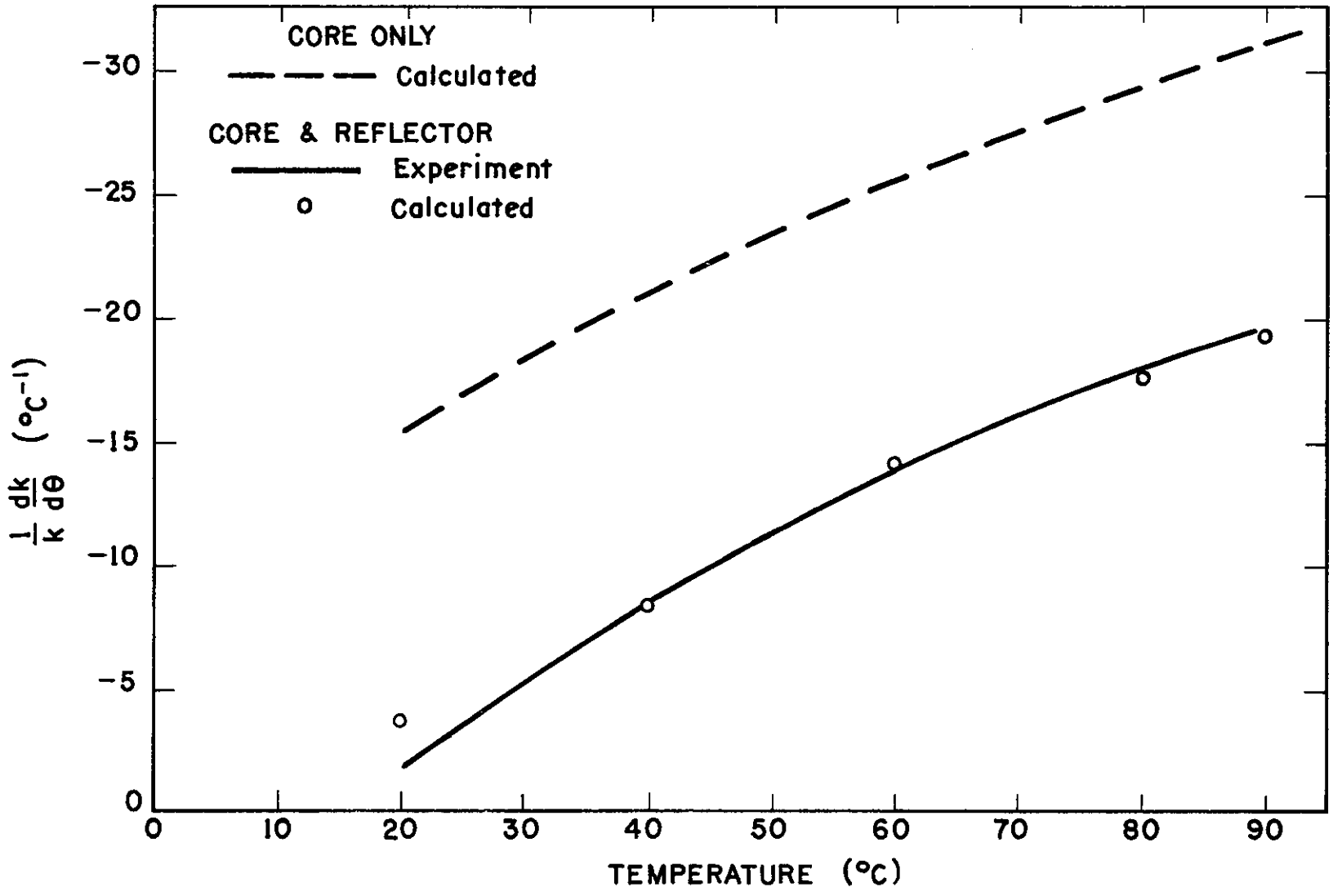

FIGURE 10. TEMPERATURE COEFFICIENT OF REACTIVITY, CORE P18/19

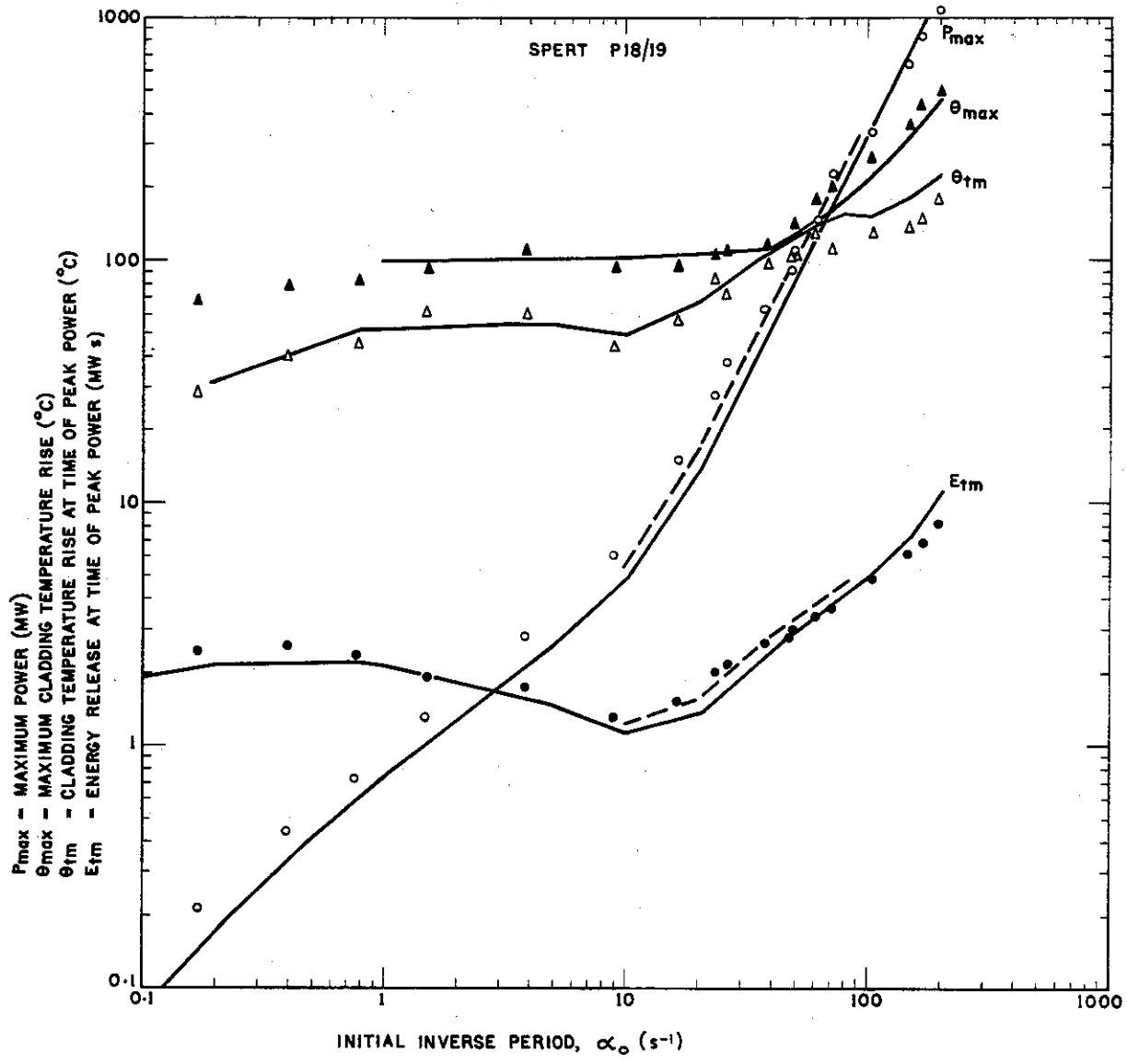

FIGURE 11. CALCULATED AND EXPERIMENTAL TRANSIENT DATA, CORE P18/19

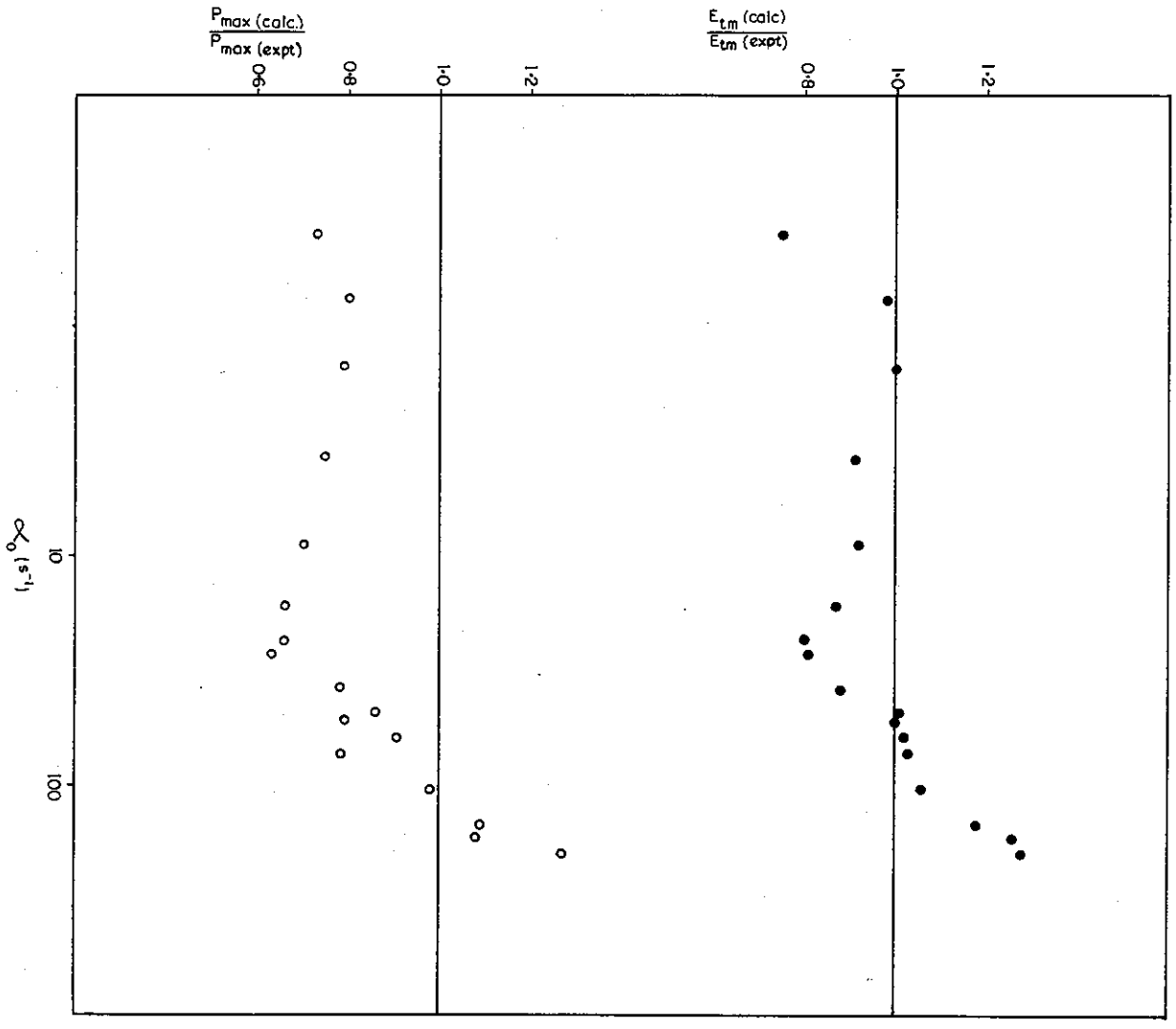

FIGURE 12. RATIOS OF MEASURED AND CALCULATED ENERGY RELEASES AND PEAK POWERS, CORE P18/19

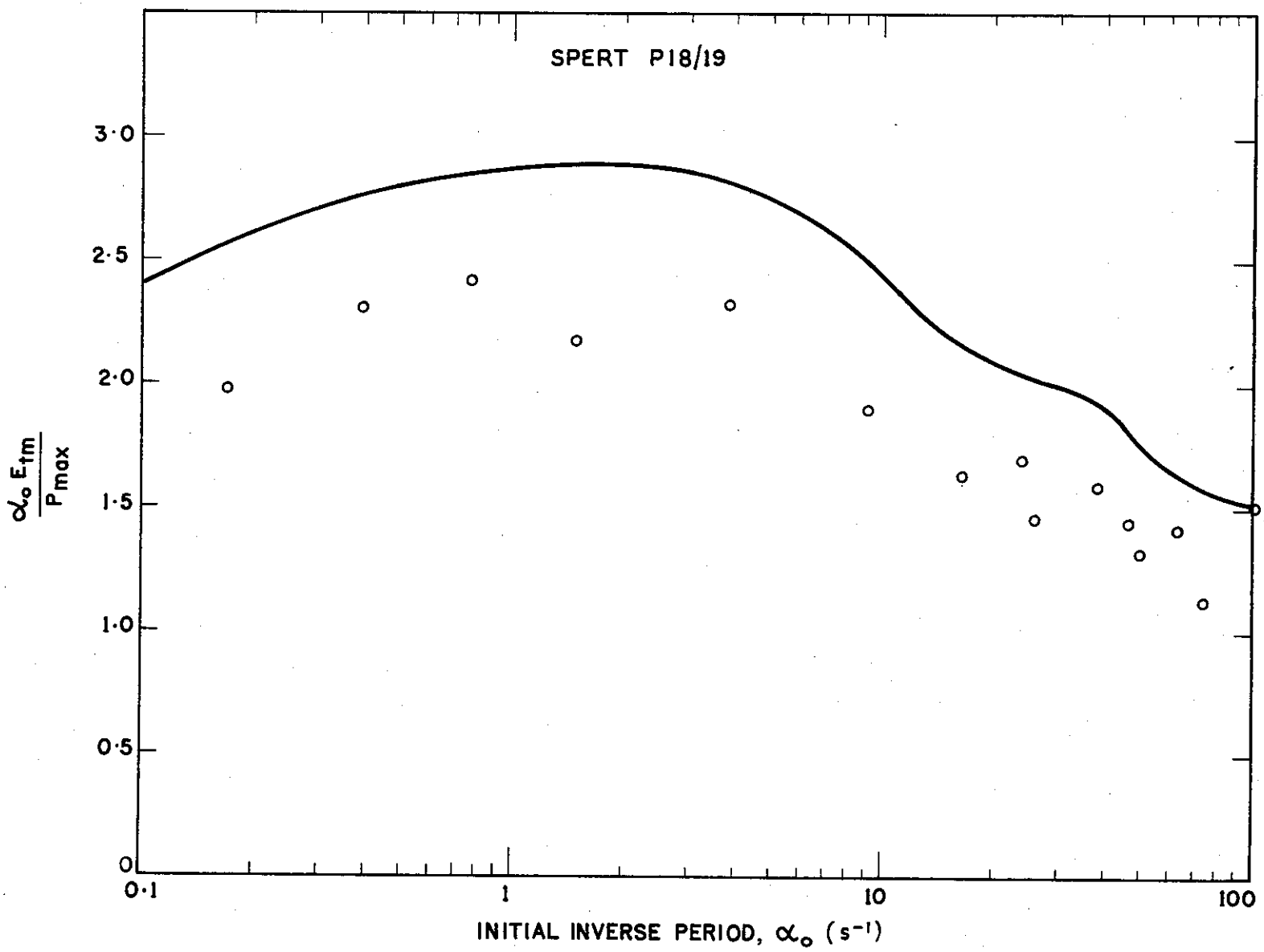

FIGURE 13. BURST SHAPES TO TIME OF PEAK POWER, CORE P18/19

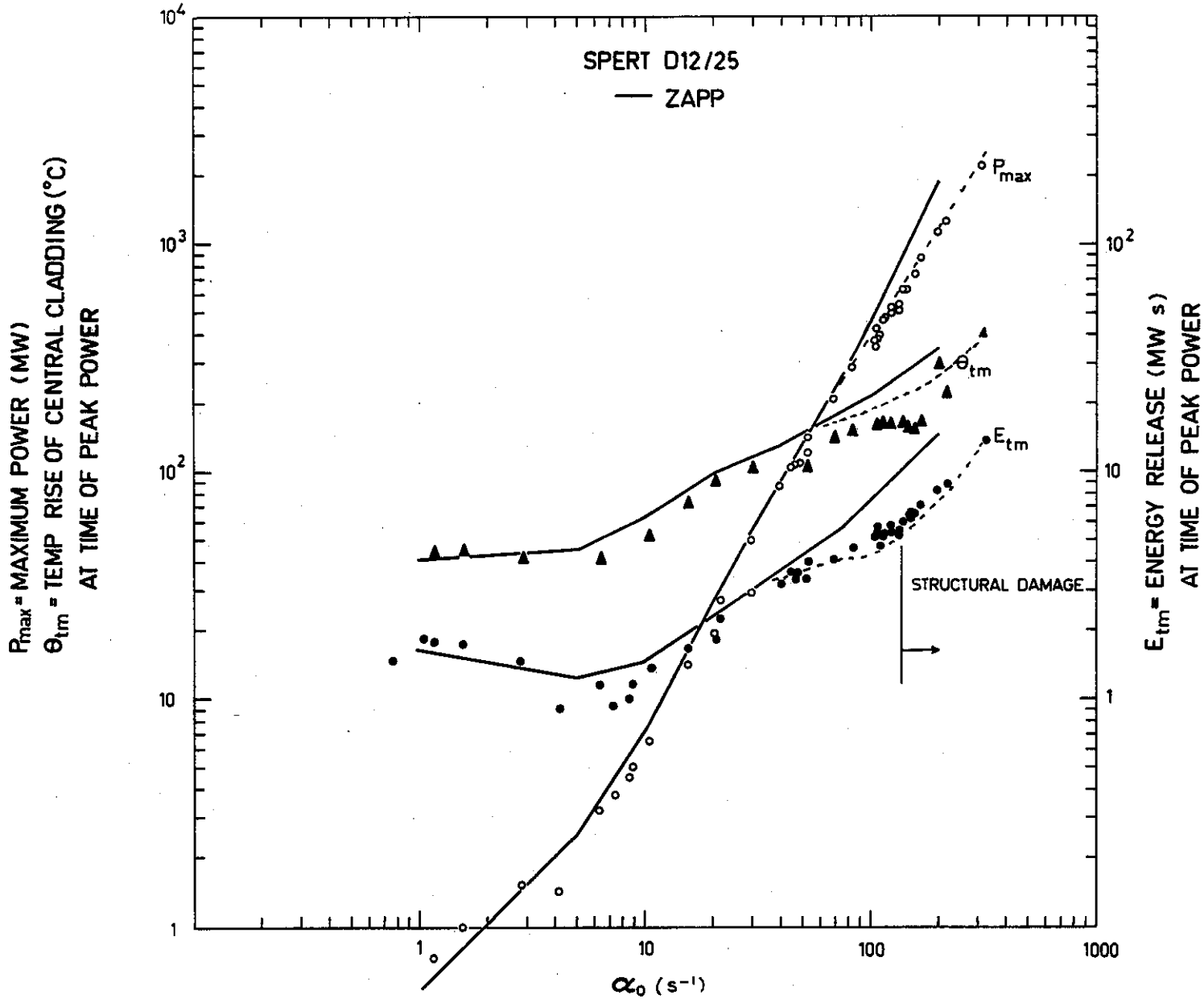

FIGURE 14. CALCULATED AND EXPERIMENTAL TRANSIENT DATA, CORE D12/25

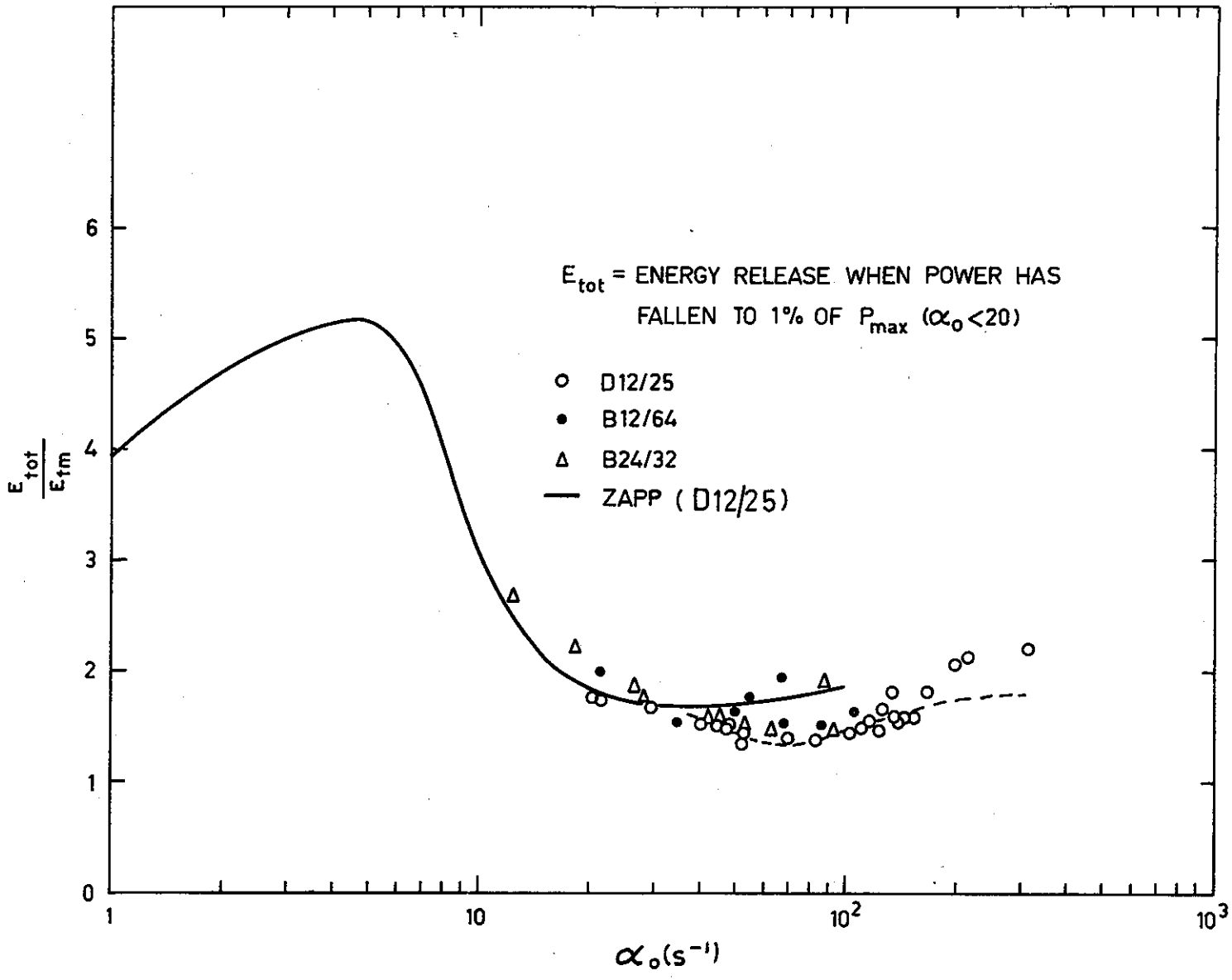

FIGURE 15. BURST SHAPE ASYMMETRY, CORE D12/25